Chapter 3

# Sintering Prealloyed Powders Fe-Ni-Cu-Mo Modified by Boron Base on Thermodynamic Investigations

Joanna Karwan-Baczewska and Bogusław Onderka

Additional information is available at the end of the chapter

http://dx.doi.org/10.5772/66875

**Abstract**

One of the methods to reduce porosity and increase mechanical properties of Fe-Ni-Cu-Mo powder type is applying activated sintering with the boron powder. In the experiments, a diffusion bonded prealloyed powder type Distaloy SA (Fe-1.75%, Ni-1.5%, Cu-0.5%, Mo) was used alloyed by 0.2, 0.4, and 0.6 mas.% elemental boron powder with the addition of 0.8 mas.% of zinc stearate lubricant. Powders were 15 min blended, compacted and then sintered. The sintering process was elaborated in detail based on microstructure investigations and thermodynamic analysis, which showed that the liquid phase has to be formed as a result of eutectic reaction between matrix elements (Fe, Mo, Ni) and mixed boride $(Fe, Mo, Ni)_2B$. In alloys with boron excess, the liquid phase may occur already a 1176°C in conformity with the reaction: $L \leftrightarrow \gamma\text{-Fe} + Fe_2B$. Its quantity is increased with liquid solution formed in the eutectic reaction running between boron and copper at 1027°C. If the system tends to be in equilibrium, the chemical composition of the liquid solution should be shifted toward higher Fe levels.

**Keywords:** prealloyed Fe-Ni-Cu-Mo powder, boron, liquid phase sintering

## 1. Introduction

The knowledge of thermodynamic properties of the B-Fe system was successfully applied in several branches of materials engineering, e.g., B-Fe is a subsystem in B-Fe-Nd alloys characterized with strong magnetic properties [1, 2] and in B-Fe-Ti-based composite alloys strengthened by $TiB_2$ [3]. In addition, boron is used as an alloying element in order to enhance steel hardenability and to produce amorphous alloys [4–6].

For interesting technological parameters, iron-based alloy systems were a subject to intensive research and theoretical investigations [7–20] and so were materials made from premelting of powders from the Fe-Mo system with max. 1.5% Mo [21–25].

With respect to the final density, alloy compositions, used quantity of boron, and other additions, the properties of Fe-Mo alloys improved [26, 27]. However, in some studies on this system [21, 28], relatively poor plastic properties (ductility) were observed.

The first papers analyzing the sintering processes occurring in Fe-2.5% Mo-B alloys—with particular emphasis laid on the microstructural evolution—were published by Sarasola and co-workers [29, 30]. According to these papers, in the sintering process of Fe-3.5% Mo 0.3% powder, some boron atoms form residues around Fe powder grains at temperatures as low as 800°C through surface diffusion in the solid state. Iron particles exhibit a polycrystalline structure (SEM investigations) formed from equiaxial ferrite grains (sized 2–50 μm). At temperatures of 1000–1100°C a more complex microstructure with vast phase deposits occurs. A gradual increase in precipitation is observed as temperature rises. Such a process starts on the surface of particles, around pores and develops on grain boundaries of ferrite crystallites. In turn, the precipitation related to the diffusion of boron from the crystallites' surface toward their lattice occurs inside the crystals. Also worth mentioning is that the process of precipitation occurs at the latest in the biggest metallic particles for the longest path of diffusion.

The described microstructure exists also at a higher temperature (i.e., 1200°C), but obtained precipitations are larger and arranged more uniformly. It should be stressed that not only all processes occurred in the solid phase, but also no traces of liquid phase were observed even at temperatures 25°C over the eutectic: $L \leftrightarrow \gamma\text{-Fe} + Fe_2B$ (1176°C).

The microstructure of material subject to sintering at 1230°C and registered by means of SEM (scanning electron microscopy) method [29, 30] exhibits a clear reduction of the number of precipitations with larger, dark areas of liquid solution of eutectic composition which is surrounded by distinct envelopes identified as the metallic matrix of an alloy with a lower Fe/Mo ratio. Such a process can continue even to 1280°C. Microphotographs of samples held at 1230 and 1280°C indicated that liquid phase areas could also exist on the surface of particles, on the boundaries of ferrite grains, nearby pores, and in Fe grain matrix viz. in places where precipitations were noticed.

While comparing the evolution of microstructure in the Fe-B and Fe 3.5% Mo-0.3% B alloys, it can be stated that the microstructure of Fe-Mo-B alloys after a heat treatment at 1000°C had revealed big quantities of clearly marked inclusions absent in the Fe-B system [29, 30]. In addition, the liquid solution in the Fe 3.5% Mo 0.3% B alloys appeared at a temperature higher than in the system Fe-B where the advanced sintering process was already observed at the eutectic temperature (1176°C) (**Figure 1**).

Moreover, the microstructure of Fe-B samples sintered at 1280°C exhibited a typical, well-developed microstructures of samples sintered with contribution from the liquid phase, whereas in the Fe 3.5% Mo-B alloys such microstructures were merely visible. An advanced

http://dx.doi.org/10.5772/66875

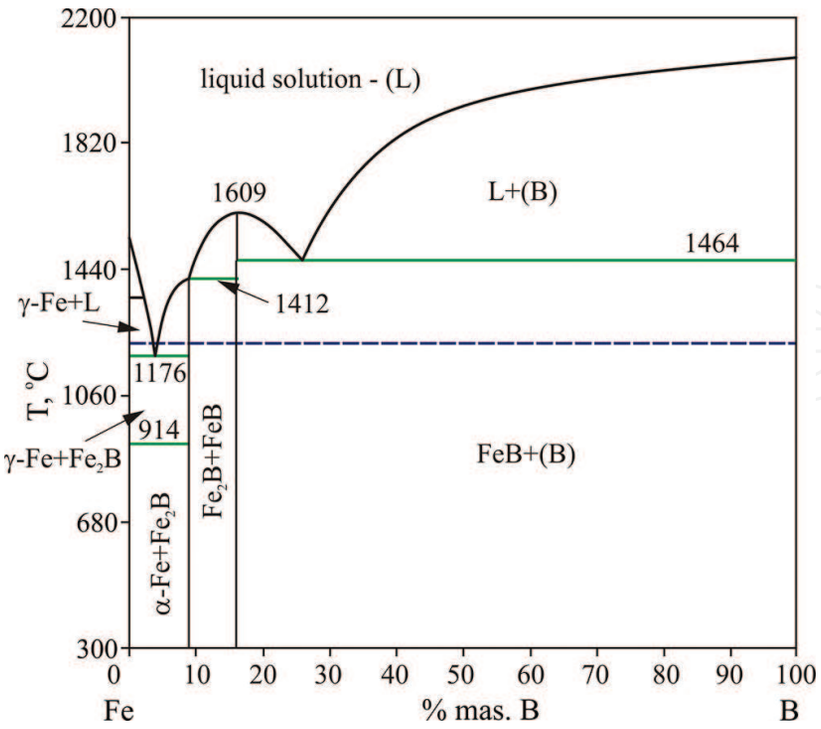


**Figure 1.** Phase equilibrium diagram Fe-B calculated according to the model parameters assessed by Hallemans and co-workers [31]. A dashed line in the diagram represents the temperature of sintering process (1200°C).

sintering process was observed—like in the Fe-B system—already at 1176°C in alloys with lower molybdenum contents in which the solidified liquid phase was noticed, too.

## 2. Experimental procedure and discussion

In the current experiments a diffusion-bonded prealloyed powder of Distaloy SA (Fe-1.75%, Ni-1.5%, Cu-0.5%, Mo) was applied. Distaloy SA powder was alloyed with the addition of 0.2, 0.4, and 0.6 mas.% of elemental boron powder with the addition of 0.8 mas.% of zinc stearate lubricant. After 15 min of blending the powder samples were compacted at 600 MPa, and then sintered for 60 min in a hydrogen gaseous envelope at 1200°C. Microstructure and the mechanical properties were investigated.

The sintering process was elaborated based on thermodynamic studies of Sarasola et al. [30]. In order to reduce the melting point of the Fe-Mo-B alloy, some quantities of Ni and Cu were also added. Copper and boron form a eutectic solution at 1027°C [32]) whose composition is strongly shifted toward Cu (97.5 mas.%) (**Figure 2**). Boron with the iron, molybdenum, and nickel (**Figures 1**, **3**, and **4a**, **b**) forms $M_2B$ type borides.

A possibility of forecasting the effect of alloy additions is very important for understanding the sintering process in multicomponent alloys Fe-Mo-Ni-Cu-B. Small amounts of alloyed doping additions do not shift the equilibrium in a five-component alloy toward the Mo-Ni

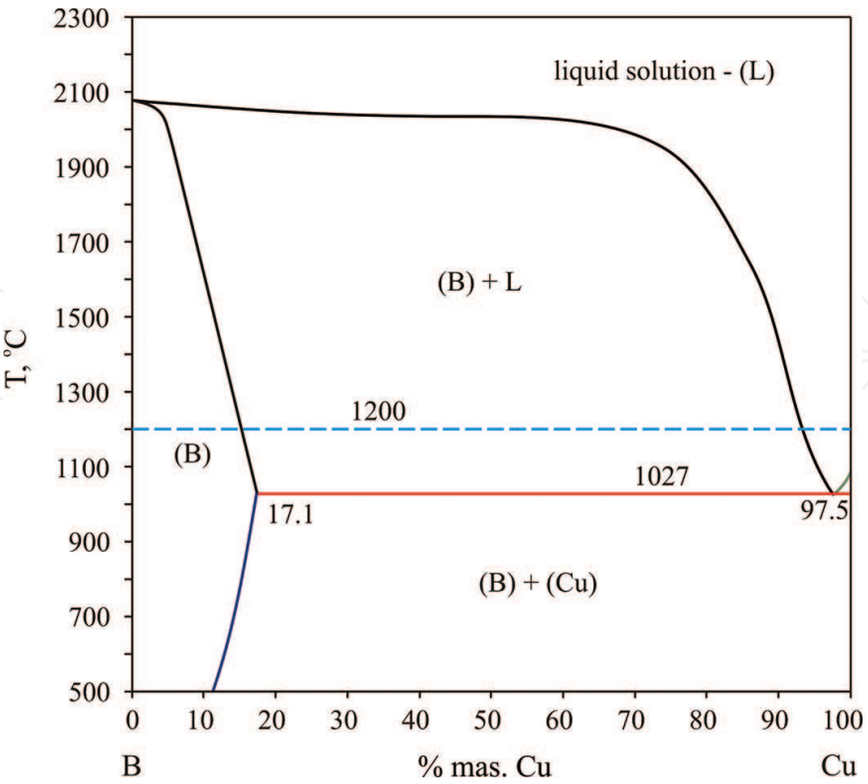


**Figure 2.** Phase equilibrium diagram of B-Cu system calculated from the assessed parameters of Zhang and co-workers [33]. Dashed line represents the sintering process temperature at 1200°C.

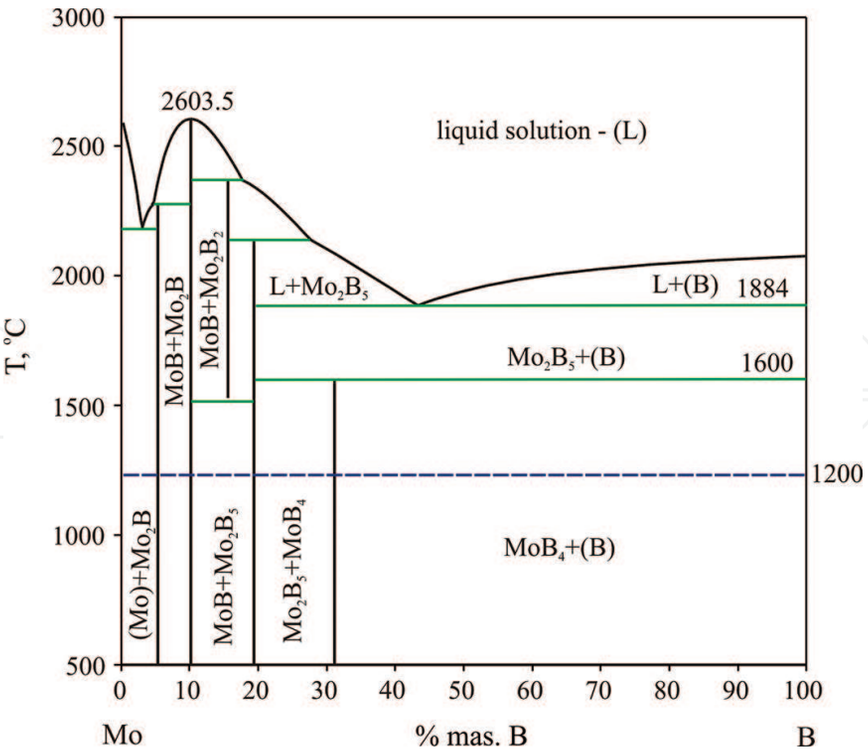


**Figure 3.** Phase equilibrium diagram of B-Mo system calculated from the model parameters determined by Morishita and co-workers [34]. Dashed line represents the sintering process temperature (1200°C).

http://dx.doi.org/10.5772/66875

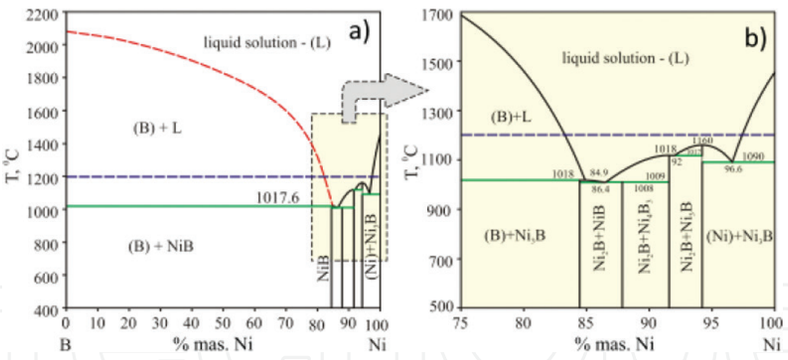


**Figure 4.** Equilibrium phase diagram of B-Ni system calculated according to the SGTE SSOL 5 Database - (a) and enlarged segment of the B-Ni system - (b). Dashed line - the sintering 1200°C temperature.

system, viz. there is no precipitation of brittle intermetallic compounds, formed in this system. Additionally, it should be mentioned that the sintering temperature of 1200°C is higher than the temperatures of congruent melting of nickel borides (**Figure 4**).

If samples are subject of rapid cooling, in the systems Ni-B and Fe-B, the primary crystallization is suppressed; then, the precipitations of metastable phases were found with a stable eutectic. Those phases are, respectively, $Ni_{23}B_6$ and $Fe_3B$ whose entropy and enthalpy of formation were assessed [4]. The calculated excess specific heat of the liquid eutectic follows the trend of formation of metallic glasses.

The formation of metastable phases implies the solidification of the eutectic whose concentration is shifted toward the equilibrium eutectic, e.g., metastable eutectic between Ni and $Ni_2B$ at 858°C and liquid concentration at 4.39 mas.% B.

The decisive effect upon the iron-rich portion of the Fe-Mo-Ni-Cu-B system is exerted by the properties of the Fe-Mo-Ni system. According to Sarasola et al. [29, 30], an appreciable portion of molybdenum which is initially in solid solution first reacts with boron and then forms a molybdenum-rich boride that is stable over 1200°C. So, the presence of molybdenum in the alloy powder leads to formation of its mixed borides, mainly $(Fe, Mo)_2B$.

Although the occurrence of $(Fe, Mo)_2B$ was not confirmed through experimental result (small XRD peaks, inaccuracy in the chemical analysis of boron with EDS and SEM), intermediate observations confirmed precipitations of this boride. First of all, over 1776°C, such precipitations were observed only when sintering powders contained 3.5 mas.% Mo [29, 30]. At lower temperatures at a constant level of boron, the quantity of such precipitations increased as molybdenum concentration rose. Secondly, the formation of a liquid phase at 1176°C was noticed during sintering of Fe-B and Fe-Mo-B powders with Mo/B atomic ratios equal 0.29 and 0.89. In opposite, no traces of liquid solution in the alloy Fe 3.5% Mo-B, with the Mo/B atomic ratio equal to 1.316 were found. Therefore, it may be concluded that when the ratio of atoms Mo to B in the alloy approaches the value of $Mo_2B$ stoichiometry the borides produced by sintering are richer in molybdenum, and at the same time, the quantity of boron which participates in the eutectic reaction at that temperature diminishes. Additionally, $Mo_2B$ and $Fe_2B$ borides are iso-structural; so in consequence, the mixed boride $(Fe, Mo)_2B$ is likely to

be formed through reciprocal substitution of Fe and Mo (solid solution) in the entire range from $Fe_2B$ to $Mo_2B$. In addition, it must be added that Gibbs free energy of formation of $M_2B$ borides containing Fe and Mo is more negative than the free energy of $Fe_2B$, and $Mo_2B$ cannot occur individually in thermodynamic equilibrium upon entering into contact with a Fe-based solution [30].

To understand the modifying effect of Mo, Cu, and Ni in the Fe-Mo-Ni-Cu-B system, one can compare phase diagrams calculated for the Fe-Mo-B system and a part of the five-component Fe-Mo-Ni-Cu-B phase diagram calculated at 1200°C by means of ThermoCalc software [32, 35]. Such calculations may be performed assuming that the solid solution of borides $(Fe, Mo, Ni)_2B$ can be described by means of the ideal solution model.

The lack of data for alloys containing boron in thermodynamic databases does not allow to calculate accurate isothermal sections for the Fe-Mo-B and Fe-Mo-Ni-Cu-B systems. That is why some parameters in thermodynamic models have to be assumed or assessed *a priori*.

Isothermal sections were calculated using the thermodynamic assessments of binary systems, available in the pertinent literature, i.e., B-Cu [33], B-Fe [31], B-Mo [34], Fe-Mo [36], Mo-Ni [37] and B-Ni, Fe-Ni, Cu-Fe, Cu-Ni, and Cu-Mo [32].

In the following thermodynamic description of the Fe-Mo-Ni-Cu-B system it was assumed that four types of phases are present in the iron-rich part of phase system: liquid phase—L, iron-based solid solutions ($\alpha$-Fe (bcc) $\gamma$-Fe (fcc) and $\delta$-Fe(bcc)) $M_2B$ type boride.

Other phases occurring in the two-component systems, like FeB, MoB, and NiB borides [38] and a few phases from the Fe-Mo-Ni system were omitted because they do not occur in the temperature and composition ranges of investigation. The three-component phase $B_2FeMo_2$ described by Gladyshevsky and coworkers [39] was also omitted as no thermodynamic data or stability ranges are available in the literature. Neither was the phase $B_5Fe_{13}Mo_2$ taken into consideration (Haschke and others [40]) because its occurrence had not been confirmed.

Liquid solution (L) and solid terminal solutions $\alpha$-Fe, $\gamma$-Fe and $\delta$-Fe were described as substitutional solution of atoms on one sublattice. The Gibbs free energy of such a model can be written in the form:

$$\begin{aligned} G^{\theta} &= x_B^0 G_B^{\theta} + x_{Fe}^0 G_{Fe}^{\theta} + x_{Mo}^0 G_{Mo}^{\theta} + x_{Ni}^0 G_{Ni}^{\theta} + x_{Cu}^0 G_{Cu}^{\theta} + \\ &RT\left(x_B \ln x_B + x_{Fe} \ln x_{Fe} + x_{Mo} \ln x_{Mo} + x_{Ni} \ln x_{Ni} + x_{Cu} \ln x_{Cu}\right) + G^{ex} + G^{mo} \end{aligned} \quad (1)$$

where excess Gibbs free energy, $G^{ex}$, can be expressed by formula:

$$\begin{aligned} G^{ex} &= x_B x_{Fe} L_{B,Fe}^{\theta} + x_B x_{Mo} L_{B,Mo}^{\theta} + x_B x_{Ni} L_{B,Ni}^{\theta} + x_B x_{Cu} L_{B,Cu}^{\theta} + x_{Fe} x_{Mo} L_{B,Mo}^{\theta} + \\ &x_{Fe} x_{Ni} L_{Fe,Ni}^{\theta} + x_{Fe} x_{Cu} L_{Fe,Cu}^{\theta} + x_{Mo} x_{Ni} L_{Mo,Ni}^{\theta} + x_{Mo} x_{Cu} L_{Mo,Cu}^{\theta} + x_{Ni} x_{Cu} L_{Ni,Cu}^{\theta} \end{aligned} \quad (2)$$

The parameters for the substitutional solution $L_{ij}$ depend on the alloy composition according to Redlich-Kister equation:

http://dx.doi.org/10.5772/66875

$$L_{i,j} = \sum_{k=0}^{n} L_{i,j}^{(k)} \left(x_i - x_j\right)^k \tag{3}$$

where parameters $L_{i,j}^{(k)}$ are the functions of temperature:

$$L_{i,j}^{(k)} = A + BT + C \cdot T \cdot \ln T + \ldots \tag{4}$$

$G_i^{\theta}$ is the Gibbs free energy of pure component (element) $i$ in the phase $\theta$, and term $G^{mo}$ represents the contribution from the magnetic order as postulated by Hillert and Jarl [41].

The borides $Fe_2B$, $Mo_2B$, and $Ni_2B$ have an identical crystal structure, so the tetragonal phase of type $M_2B$ (mixed boride) was described as a phase consisting of two sublattices (Fe, Mo, Ni)$_{0.667}$B$_{0.333}$. The lack of interactions between Fe, Mo, and Ni on the first sublattice was assumed. In line with the chosen model, Gibbs free energy of such phase can be expressed with the following formula:

$$G^{M_2B} = y_{Fe}\,{}^{0}G_{Fe_2B} + y_{Mo}\,{}^{0}G_{Mo_2B} + y_{Ni}\,{}^{0}G_{Ni_2B} + RT\left(y_{Fe}\ln y_{Fe} + y_{Mo}\ \ln\ y_{Mo} + y_{Ni}\ln\ y_{Ni}\right) \tag{5}$$

where: $y_{Fe}$ $y_{Mo}$ and $y_{Ni}$ are the site fraction of Fe, Mo and Ni in the first sublattice, respectively

Parameter ${}^{0}G_{Fe_2B}$ was taken from the work of Hallemans et al. [31], whereas ${}^{0}G_{Mo_2B}$ and ${}^{0}G_{Ni_2B}$ from the database SGTE SSOL 5 [32].

Initially, the isothermal section for 1200°C for the Fe-Mo-B system was subject to analysis. The equilibrium between liquid phase (L) and phase γ-Fe (fcc) and the iron-rich $M_2B$ type phase (Fe, Mo)$_2$B was calculated and shown in **Figure 5**. So, at that temperature, the formation of a liquid phase is connected with the presence of such a boride. At lower Mo concentrations, that

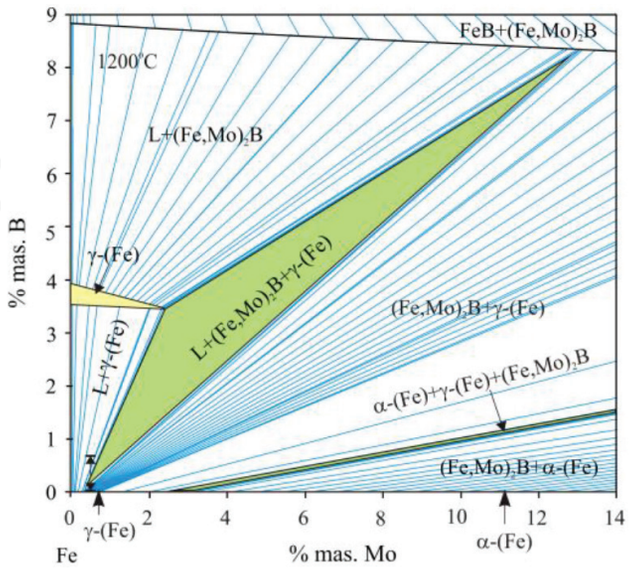


**Figure 5.** Iron-rich part of phase diagram of Fe-Mo-B system at 1200°C. Blue lines represent tie lines—lines of constant chemical potential of components of phases in equilibrium.

boride seems not occur in samples sintered at 1200°C, because in that area the liquid solution remains in equilibrium only with γ-Fe (fcc).

According to analysis of isothermal sections at 1200 and 1280°C presented in papers [29, 30], as temperature rises, the equilibrium between the Fe solid solution, liquid solution, and mixed boride $(Fe, Mo)_2B$ shifts toward higher molybdenum contents in those three phases, which means that with increasing temperature, there will be settled an equilibrium between the liquid phase, α-Fe (bcc) richer in Mo, and Mo-rich $(Fe, Mo)_2B$ phase (**Figure 5**).

Therefore, at each temperature within this range, a liquid phase is likely to occur at interface between the boride and the surrounding matrix under two conditions:

- the composition of the initial boride $(Fe,Mo)_2B$ is such that it can enter into the eutectic reaction;
- the initially precipitated Mo-based boron becomes rich in iron.

It can be thus ascertained that in comparison with the Fe-B system, a molybdenum addition will increase the eutectic temperature because a more stable boride $(Fe,Mo)_2B$ and (Fe,Mo) solution participate in the reaction. This conclusion is confirmed by the calculations on the sections of the phase diagram (**Figure 6**) where the temperature of eutectic increases in a con-

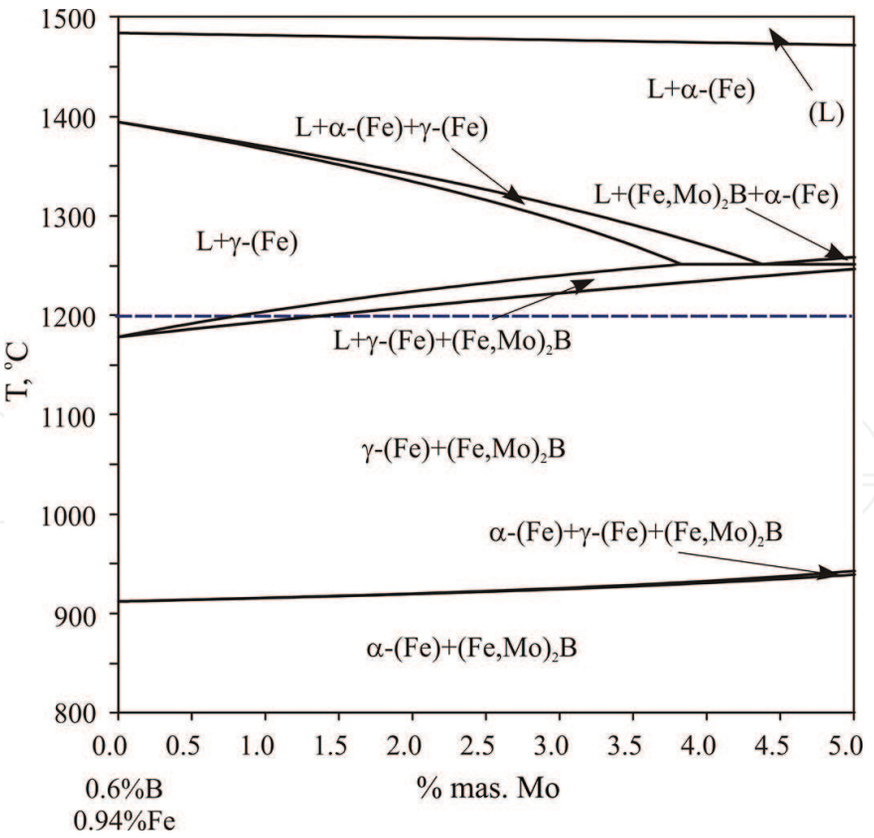


**Figure 6.** Section (isopleth) of phase diagram of the Fe-Mo-B system for 0.6% B. Letter L denotes liquid solution, and dashed line—sintering temperature 1200°C.

http://dx.doi.org/10.5772/66875

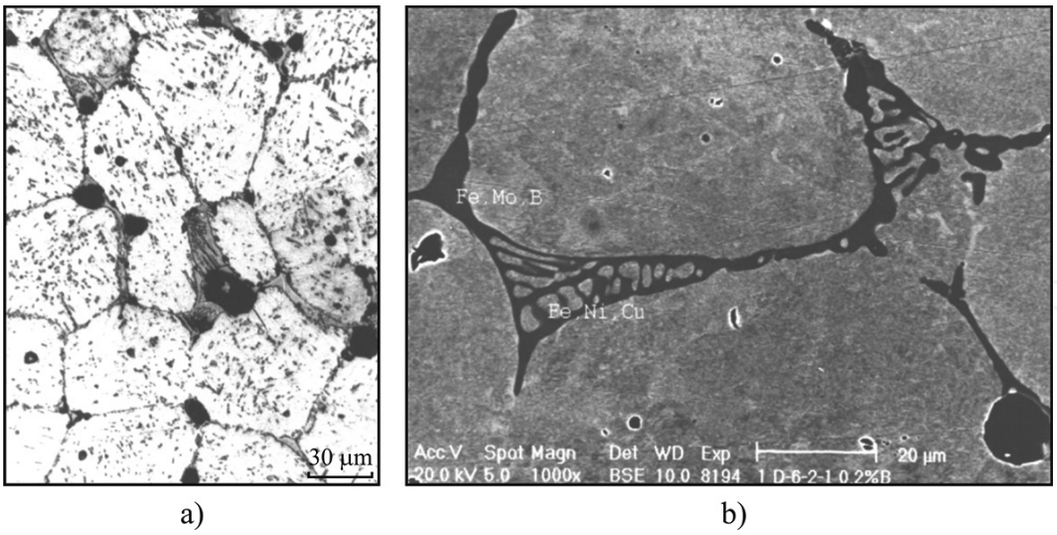


**Figure 7.** Microstructure of Distaloy SA sinters with 0.6 mas.% B (a) light microscope, (b) SEM/EDX.

tinuous way when the Mo/Fe ratio in $(Fe,Mo)_2B$ boride increases, and this reaction causes at the same time a reduction of the Fe/Mo ratio in the matrix surrounding the boride.

Such a conclusion is corroborated by experimental results pertinent to the areas of liquid phase occurring upon the grain boundaries in the alloy matrix with a reduced Fe/Mo ratio (**Figure 7a** and **b**).

For a given temperature above 1200°C (**Figure 8**), the system aimed from thermodynamic calculations may have a stability range of initial $M_2B$ borides whose composition is desired (bearing in mind the inclusion of iron from the surrounding matrix (alloy) into $M_2B$ borides,

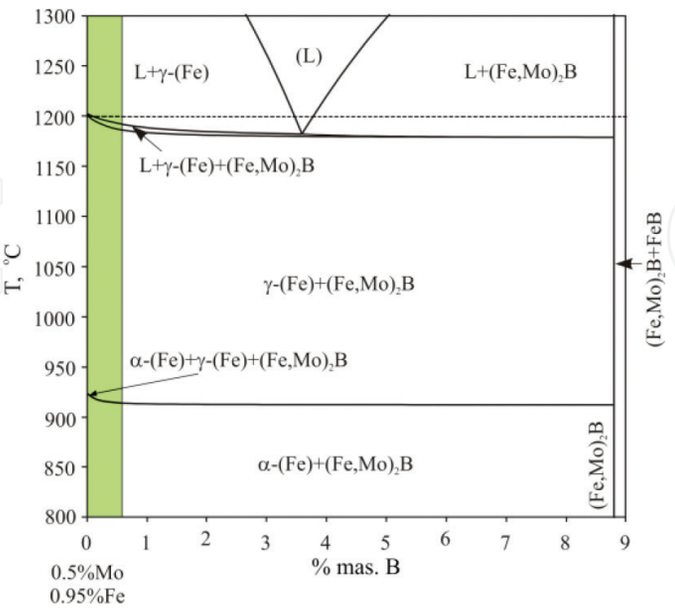


**Figure 8.** A part of section of the phase diagram of the Fe-Mo-B system at a constant Mo level (0.5 mas.%). Green color denotes the boron concentration range examined in this study (0–0.6 mas.%).

which will at the same time lead to an increase in the matrix Mo/Fe ratio. Such a process is thermodynamically justified and leads to the stabilization of the driving force of the Fe diffusion into boride $(Fe,Mo)_2B$. Its effect is that the areas in which the liquid solution comes to exist become poorer and poorer in Fe.

An alternative to Mo diffusion from borides to the surrounding matrix is related with a higher stability of Mo containing borides when compared to Fe-based borides. It can be assumed [30] that as iron-enriching process proceeds in the initially precipitated borides with a high Mo level, there will be settled a flow of Fe atoms moving toward those borides. In consequence, a complex concentration gradient within the grains of the matrix solid Fe-Mo will be formed solid along grain boundaries and around pores. Such an unbalanced flow of atom is simultaneously accompanied by the production of a small quantity of spheroid pores in the alloy matrix (the so-called secondary porosity) (**Figure 7**), which is caused by Kirkendall effect.

If the sintering process continues to be thermally activated, the occurrence of the liquid phase contributes to a more and more accurate determination (demarcation) of grain boundaries and the chemical gradient starts to diminish. Such microstructural changes are connected with a comprehensive trend followed by the system which moves toward an equilibrium, viz. to a phase composition resulting from the total input alloy concentration.

Analyzing a part of the section of the Fe-Mo-B system for a constant level of 0.5 mas.% Mo, it can be found out that only in the initial stage of boron addition to the Fe-0.5% Mo alloy a fall in temperature is recorded when a liquid phase comes to exist (three phase equilibrium, viz. L + γ-Fe + $(Fe, Mo)_2B$). Over 1.5 mas.% B, the temperature no longer depends on the boron concentration (**Figure 8**—plateau).

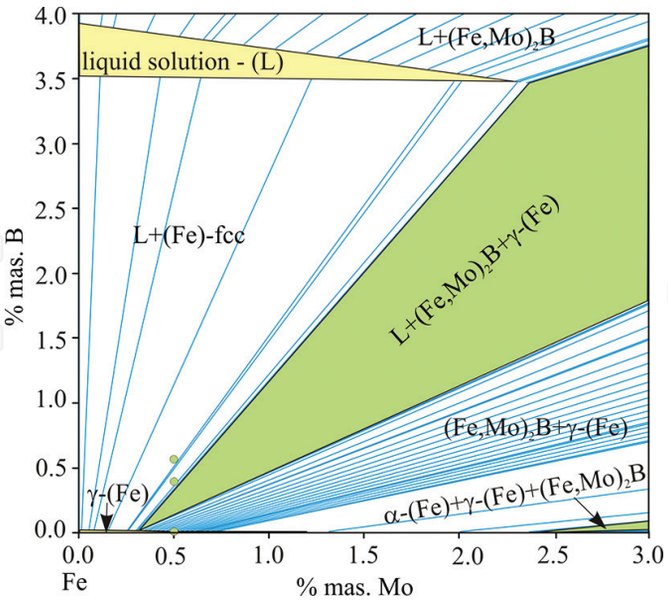


**Figure 9.** Enlargement of an iron-rich part of the Fe-Mo-B phase diagram at 1200°C; tie lines are marked in blue. Green points stand for compositions of samples subject to sintering.

http://dx.doi.org/10.5772/66875

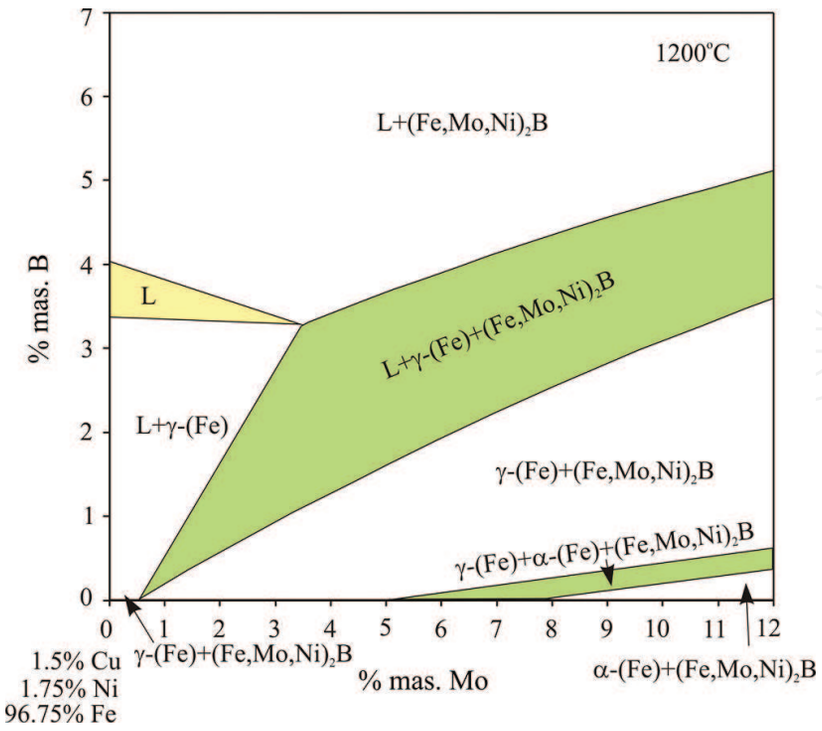


**Figure 10.** Phase diagram of iron-rich portion of phase diagram Fe-Mo-Ni-Cu-B calculated for 1.5 mas.% Cu, 1.75 mas.% Ni at 1200°C. Dashed line stands for the range of concentrations of samples subject to sintering.

A comparison with the iron-rich phase diagram Fe-Mo-B and Fe-Mo-Ni-Cu-B (0.5 mas.% Mo, 1.75 mas.% Ni, 1.5 mas.% Cu) performed in this work at 1200°C (**Figures 9** and **10**) can indicate that primary alloy composition remain within the two-phase field *liquid solution + solid solution* (γ-Fe) only after addition of nickel and copper into Fe-Mo-B alloy. It can be proved that when the system is to reach such an equilibrium, the chemical composition of the liquid solution shifts toward higher Fe contents. In such a situation, the liquid solution accepts iron from its surroundings, which leads to the formation of local fronts in the liquid and continuity between grain interiors precipitated from the liquid and their surface. However, it should be stressed that in the case of alloys containing the boron excess, the liquid phase may occur already over 1176°C in conformity with the reaction: L ↔ γ-Fe + (Fe, Mo, Ni)$_2$B.

The last stage of microstructural development takes place when the alloy is subjected to soaking at a given temperature, and shows another (extra) reduction of chemical gradient and porosity. It seems that the mobility of grain boundaries is limited not only by differences in chemical composition on both sides of those grains, but also by the dispersion of small inclusions which immobilize grain boundaries.

Such a conclusion may be formulated based upon the evaluation of formation of sintered grain boundaries at 1280°C [29, 30]. The authors of the adduced work ascertained that even after 1 h time after the process had started, the system was still away from the equilibrium, but the final density of Mo containing alloys was equal to 7.8 g/cm$^3$. Therefore, it can be stated that a very good characteristic of wettability of the liquid phase caused the material to be thickened.

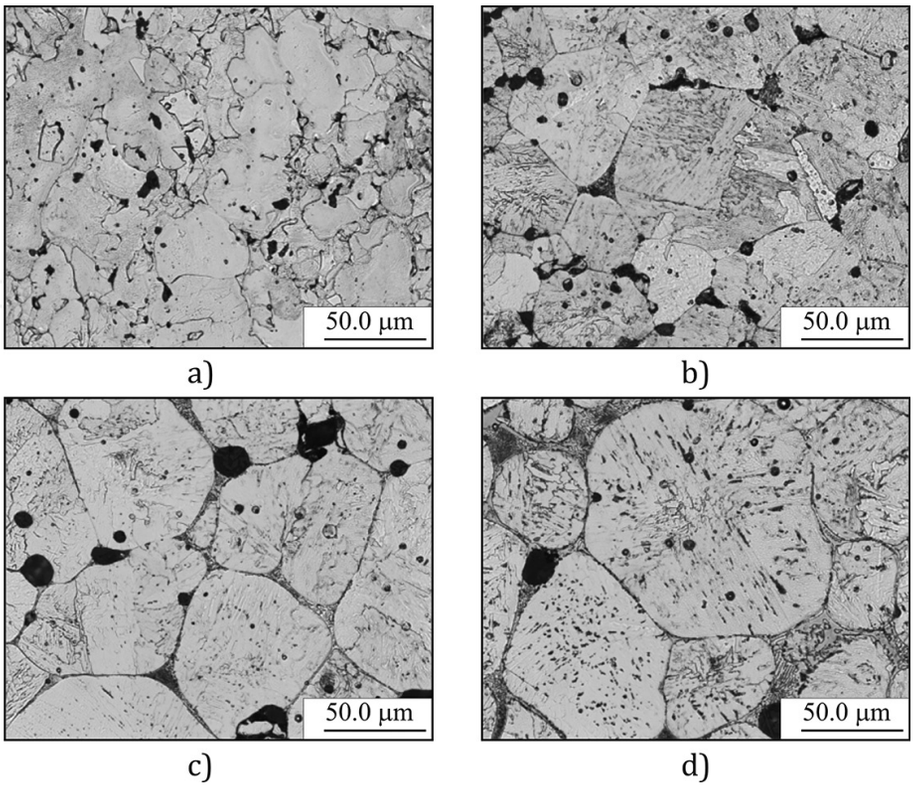


**Figure 11.** Microstructure of Distaloy SA sinters with boron addition (a) 0 mas.% B, (b) 0.2 mas.% B, (c) 0.4 mas.% B, (d) 0.6 mas.% B.

The thermodynamic analysis performed on the system Fe-0.5% Mo 1.75% Ni-1.5% Cu-B introduced to us the description of the sintering process for samples made from Distaloy SA powder with boron additions, respectively, 0.2, 0.4, and 0.6%, which matched the results of dilatometric tests and investigations into the microstructure of sinters. When Distaloy SA samples with boron addition are being heated up and soaked to 1200°C, before the liquid phase comes to exist at lower temperatures, some $M_2B$ type borides occur (in line with thermodynamic analysis) (**Figure 10**). Those phases nucleate on the surface of particles and pores as well as upon the grain boundaries of ferrite and inside it (**Figures 11b–d** and **12a** and **b**).

The liquid phase is formed as a result of eutectic reaction between matrix elements (Fe, Mo, Ni) and borides $(Fe, Mo, Ni)_2B$. In alloys with boron excess, the liquid phase may occur already at 1176°C in conformity with the eutectic reaction Fe-$Fe_2B$ (**Figure 1**). Its quantity is increased with liquid solution formed in the eutectic reaction running between boron and copper at 1013°C (**Figure 2**). Because the sinter compositions under investigation fall within the two-phase area *liquid solution + solid solution* then borides should not be in equilibrium with such phases. If the system were to attain equilibrium, the chemical composition of the liquid solution should be shifted toward higher Fe levels.

According to dilatometric tests and thermodynamic analysis, the resulting borides increase the eutectic temperature if compared with the Fe-B system where the eutectic point is 1176°C (**Figure 1**).

http://dx.doi.org/10.5772/66875

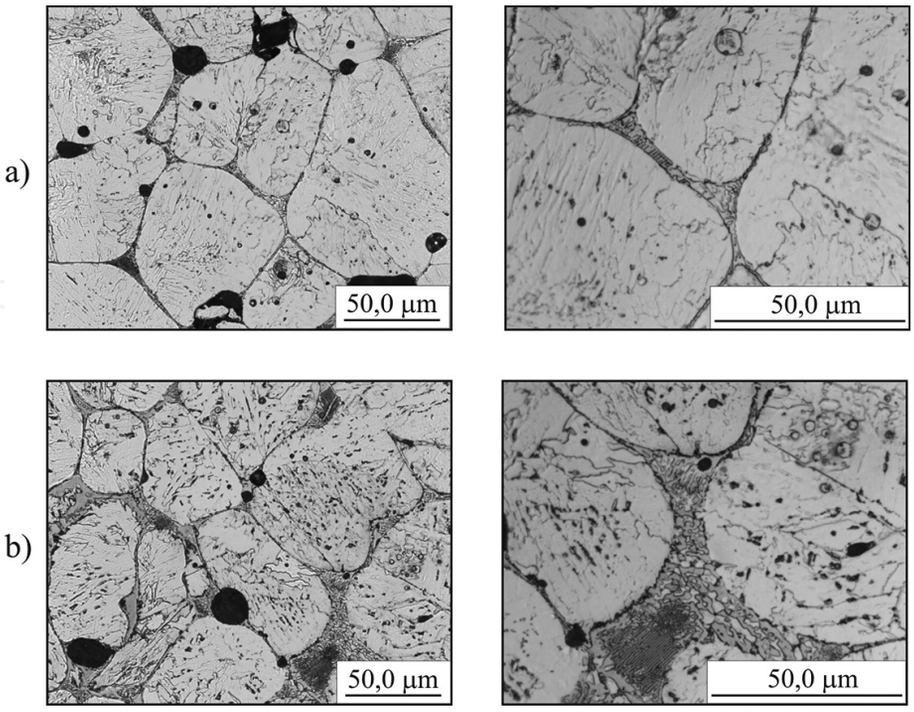


**Figure 12.** Microstructure of Distaloy SA sinters with boron addition (a) 0.4 mas.% B, (b) 0.6 mas.% B.

In addition, based upon the investigation into dilatometric curves for Distaloy SA samples, it can be stated that boron influences the process of linear contraction; the highest linear contraction was recorded at 1180°C in a Distaloy SA sample with boron 0.6 mas.% [41]. The recorded linear contraction in the sinters under investigation is connected with formation of borides and the liquid phase.

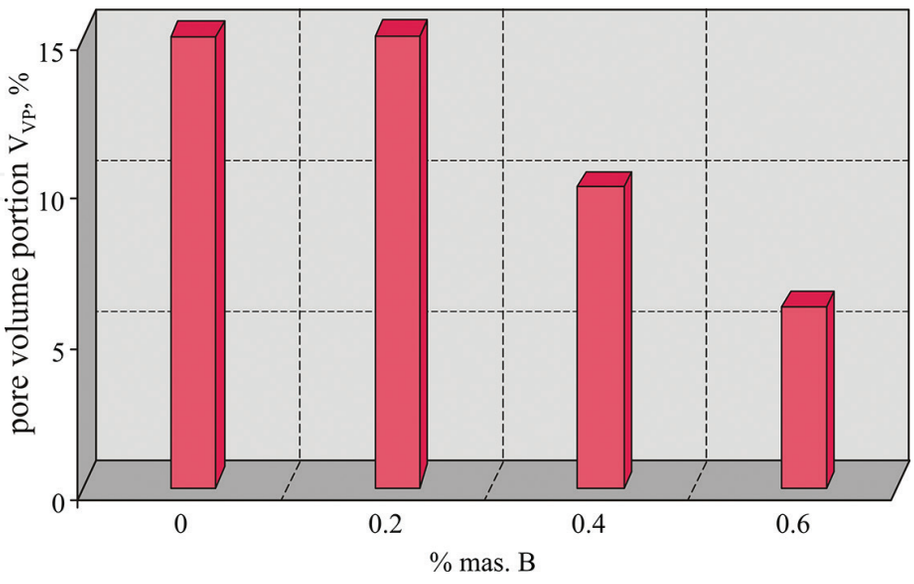


**Figure 13.** Effect of boron upon pore volume portion ($V_{vp}$) in sinters made from Distaloy SA powder. Volume portion of pores was determined through quantitative metallography. Sintering parameters: 1200°C/hydrogen/60′.

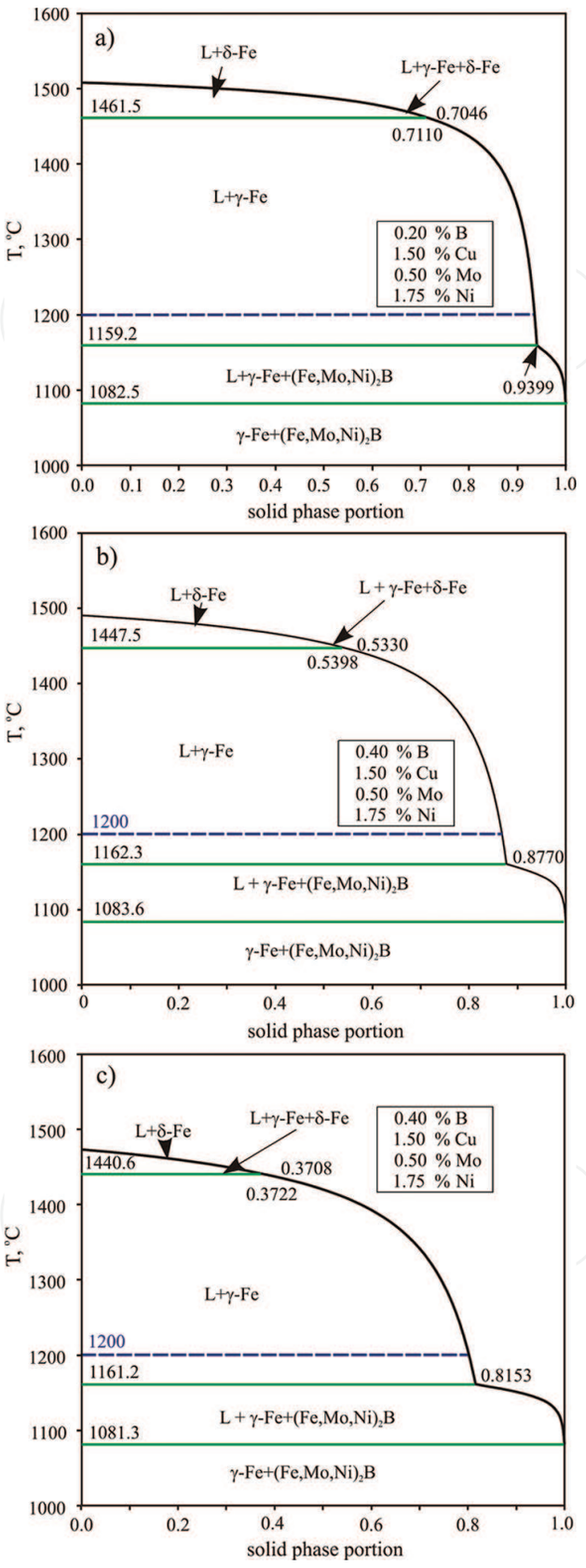


**Figure 14.** Comparison of crystallization paths for alloy Fe-1.5%, Cu-0.5%, Mo-1.75%, Ni with boron additions: (a) 0.2; (b) 0.4; and (c) 0.6 mas.%. An appreciably higher portion of liquid phase L at 1200°C and 0.6 mas.% B is visible.

http://dx.doi.org/10.5772/66875

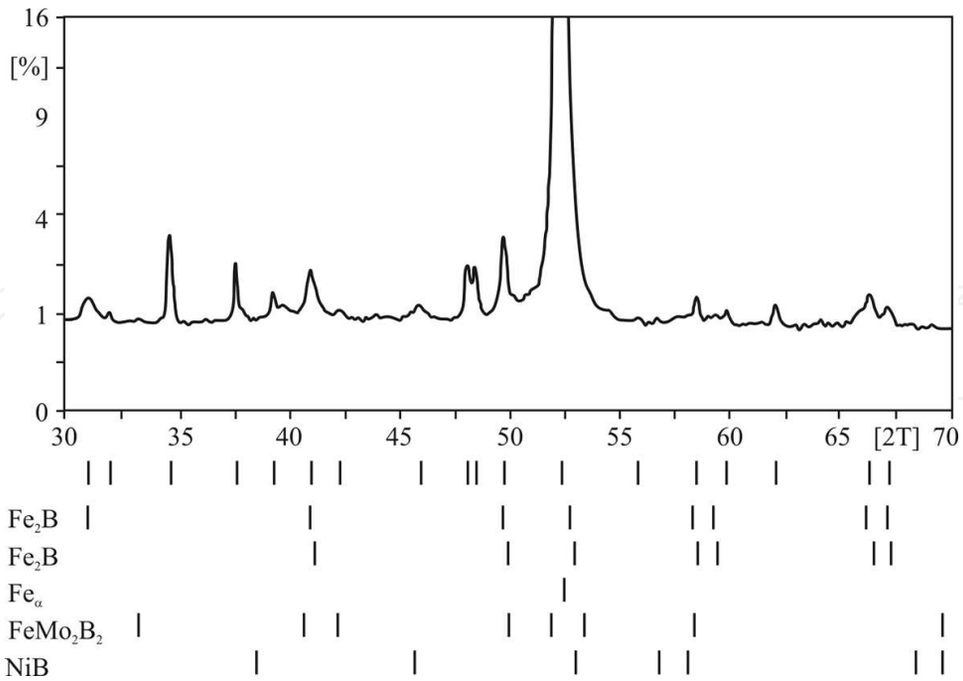


**Figure 15.** Diffraction pattern for Distaloy SA sinters with boron.

The results of observations of the microstructure in Distaloy SA samples with boron addition, subject to sintering at 1200°C, corroborate the sintering process postulated for that powder based upon thermodynamic data. Some changes in the porosity morphology (closing and spheroidization of pores), decrease in pore volume portion (**Figure 13**) and violent growth of grains were noticed, best seen at 0.6 mas.% B (**Figure 11**).

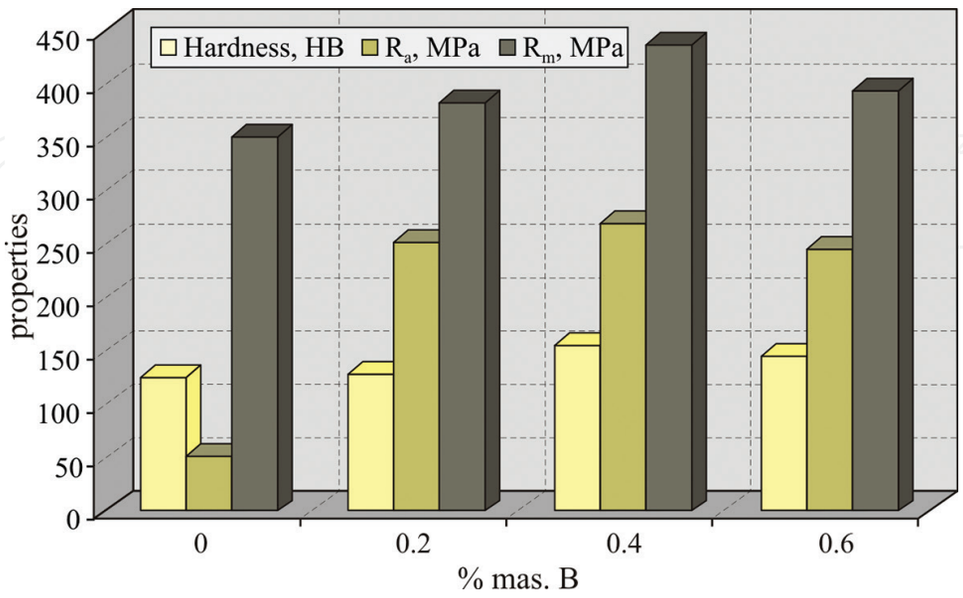


**Figure 16.** Mechanical properties of Distaloy SA sinters with boron.

An eutectic consisting of boride phases precipitates along grain boundaries of the γ-Fe phase. The composition of borides is different from predictions made through thermodynamic analysis, because during the experiment the system cannot reach the equilibrium state. As the boron contents in Distaloy SA sinters increase, an increase in the volume portion of eutectic was also observed, which is illustrated in **Figure 14** showing crystallization paths for alloy Fe-1.5% Cu-0.5% Mo-1.75% Ni with 0.2, 0.4, and 0.6 mas.% B. A larger portion of liquid phase is visible at 0.6% B.

The presence of borides in the Distaloy SA sinters with boron additions was identified by means of X-ray microanalysis and phase analysis. The following borides were found: $Fe_2B$, $FeMo_2B_2$, and NiB, and Cu (eutectic), and $FeMo_2B_2$ (matrix) (**Figure 15**) [42]. Therefore, once formed, nickel and iron borides are stable within the range of composition and temperature, subjected to investigations, and their decomposition—as the system tends toward equilibrium—is difficult to occur, which leads to a metastable state with the liquid phase of eutectic reaction, iron-based solid solution and boride phase-like $(Fe, Mo)_2B$ or $(Fe, Mo, Ni)_2B$.

The suggested sintering process in the Fe-Mo-Ni-Cu-B system favors a high degree of compaction in Distaloy SA samples.

The defined sintering process occurring in the system Fe-Mo-Ni-Cu-B is decisive for the formation of an appropriate microstructure of Distaloy SA powder with boron addition, which affects their mechanical properties. As boron contents rose in Distaloy SA samples, increases in compactness, hardness and growth of parameters $R_a$, $R_m$ were noticed (**Figure 16**).

## 3. Conclusions

(1) Those observations imply that the liquid phase participating in the sintering process of the five-component Fe-Mo-Ni-Cu-B system is characterized by very good wettability and leads to high densities.

(2) Sintering process occurring in the system Fe-Mo-Ni-Cu-B is decisive for the formation of an appropriate microstructure of Distaloy SA powder with boron addition, which affects their mechanical properties.

(3) Sintering process of prealloyed powder with boron was explained in detail on the basis of thermodynamic analysis and microstructure investigations.

## Author details

Joanna Karwan-Baczewska* and Bogusław Onderka

*Address all correspondence to: jokaba@agh.edu.pl

Faculty of Non-Ferrous Metals, AGH University of Science and Technology in Cracow, Cracow, Poland

http://dx.doi.org/10.5772/66875

## References


[1] Sagawa M, Hirosawa S, Yamamoto H, Fujimura S, Matsuura Y: Nd-Fe-B permanent magnet materials. Japanese Journal of Applied Physics. 1987; **2,** (6): 785–800.

[2] Hallemans B, Wollants P, Roos J R: Thermodynamic assessment of the Fe-Nd-B phase diagram. Journal of Phase Equilibria and Diffusion. 1995; **16,** (2): 137–149.

[3] Tanaka K, Saito T: Phase equilibria in $TiB_2$-reinforced high modulus steel. Journal of Phase Equilibria and Diffusion. 1999; **20**: 207–214.

[4] Battezzatti L, Antonione C, Baricco M: Undercooling of Ni-B and Fe-B alloys and their metastable phase diagrams. Journal of Alloys and Compounds. 1997; **247**: 164–171.

[5] Inoue A: Stabilization of metallic supercooled liquid and bulk amorphous alloys. Acta Materialia. 2000; **48**: 279–306.

[6] Palumbo M, Cacciamani G, Bosco E, Baricco M: Driving forces for crystal nucleation in Fe-B liquid and amorphous alloys. Intermetallics. 2003; **11** (11–12): 1293–1299.

[7] Witusiewicz VT: Thermodynamics of binary and ternary melts of 3d transition metals (Cr, Mn, Fe, Co and Ni) with boron. Thermochimica Acta. 1995; **264**: 41–58.

[8] Karwan-Baczewska J: Boron influence on the liquid phase sintering and the mechanical properties of P/M Distaloy alloys. Advances in Powder Metallurgy & Particulate Materials. 1996; **3** (11–15): 11–27.

[9] Karwan-Baczewska J: Boron modified materials sintered from Distaloy SA powder. Powder Metallurgy (in Polish). 1996; **29** (3/4): 18–22.

[10] Karwan-Baczewska J: Influence of boron on the structure and mechanical properties of sintered and ion-nitrided Distaloy alloys. International Journal of Materials and Product Technology. 2000; **15** (3–5): 193–204.

[11] Karwan-Baczewska J, Pieczonka T: Sintering Process of Distaloy SA and Astaloy Mo modified by boron. In: Proceedings of the Powder Metallurgy World Congress & Exhibition (World PM1998 Congress & Exhibition); 18–22 October 1998; Granada, Spain: EPMA: 1998. vol. **3**, pp. 281–286.

[12] Karwan-Baczewska J, Rosso M: Effect of boron on microstructure and mechanical properties of PM sintered and nitride steels. Powder Metallurgy. 2001; **44** (3): 221–227.

[13] Kuroki H: A review on the effect and behavior of boron in sintered iron and steel. Japan Society of Powder and Powder Metallurgy. 2001; **48** (4): 293–304.

[14] Pieczonka T, Kazior J, Płoszczak J: Dimensional changes occurring during sintering of Astaloy CrM powder compacts with boron and carbon additions. In: Proceedings of the European Congress & Exhibition on Powder Metallurgy (EuroPM 2001 Congress & Exhibition); 22–24 October 2001; Nice, France: EPMA: 2001, vol. 1, pp. 310–315.

[15] Kazior J, Pieczonka T, Płoszczak J: The influence of boron on the mechanical properties of prealloyed Astaloy CrM powders alloys. In: Proceedings of the International Conference of Deformation and Fracture in Sintered PM Materials (DF PMM); 15–18 September 2002; Stara Lesna, Slovakia: 2002, vol. 1, pp. 125–131.

[16] Marucci M, Causton R, Lawley A, Saritas S: Effect of small additions of boron on the mechanical properties and hardenability of sintered steels. Powder Metallurgy. 2002; **46** (2): 171–174.

[17] Van Rompaey T, Hari Kumar KC, Wollants P: Thermodynamics optimization of the B-Fe system. Journals of Alloys and Compounds. 2002; **334** (1–2):173–181.

[18] Tokunaga T, Ohtani H, Hasebe M: Thermodynamic evaluation of the phase equilibria and glass-forming ability of the Fe-Si-B system. Computer Coupling of Phase Diagrams and Thermochemistry. 2004; **28** (4): 354–362.

[19] Molinari A, Kazior J, Marchetti F, Canteri R, Cristofolini I, Tiziani A: Sintering mechanisms of boron alloyed AISI 316L stainless steels. Powder Metallurgy.1994; **37** (2): 115–122.

[20] Koichu H, Mitsuru N, Hiroshi H: Effect of boron and silicon additions on liquid-phase sintering behavior and corrosion resistance of P/M ferrite type stainless steels. Journal of the Japan Society of Powder and Powder Metallurgy. 2000; **47** (10): 1091–1096.

[21] German RM, Hwang KS, Madan DS: Analysis of Fe-Mo-B sintered alloys. Powder Metallurgy International.1987; **19** (2): 15–18.

[22] Dudrova E, Selecka M, Bures R, Kabatova M: Effect of boron addition on microstructure and properties of sintered Fe-1.5 Mo Powder Materials. The Iron and Steel Institute of Japan. 1997; **37** (1): 59–64.

[23] Molinari A, Pieczonka T, Kazior J, Gialanella S, Straffelini G: Dilatometry study of the sintering behavior of boron alloyed Fe-1.5% Mo Powder. Metallurgical and Material Transactions. 2000; **31A**: 1497–1506.

[24] Liu J, German RM, Cardamone A, Potter T, Semel FJ: Boron-enhanced sintering of iron-molybdenum steels. The International Journal of Powder Metallurgy. 2001; **37** (5): 39–48.

[25] Xiu Z, Salwen A, Qin X, He F, Sun X: Sintering behavior of iron-molybdenum steels with the addition of Fe-B-C master alloy powders. Powder Metallurgy. 2003; **46** (2): 171–174.

[26] Madan DS, German RM: Enhanced sintering for ferrous components. Modern Developments in Powder Metallurgy. 1986; **15**: 441–454.

[27] Madan DS, German RM, James WB: Iron-boron enhanced sintering. Progress in Powder Metallurgy. 1986; **42**: 267–283.

[28] German RM: Diffusional activated sintering - densification microstructure and mechanical properties. The International Journal of Powder Metallurgy and Powder Technology. 1983; **19**: 277–283.

[29] Sarasola M, Tojal C, Castro F: Study of boron behavior during sintering of Fe/Mo/B/C alloys to near full density. In: Euro PM2004 Conference Proceedings (Euro PM2004 Conference); 17–21 October 2004; Vienna, Austria. 2004. **3**, pp. 319–326.

[30] Sarasola M, Gomez-Acebo T, Castro F: Liquid generation during sintering of Fe-3.5% Mo powder compacts with elemental boron additions. Acta Materialia. 2004; **52** (15): 4615–4622.

[31] Hallemans B, Wollants P, Roos JR: Thermodynamic reassessment and calculation of the Fe-B phase diagram. Zeitschrift für Metallkunde.1994; **85**: 676–682.

[32] Sundman B, Shi P: SSOL5 SGTE solution database. Stockholm, Sweden, ThermoCalc Software. 2008.

[33] Zhang W-W, Du Y, Xu H, Xiong W, Kong Y, Sun W, Pan F, Tang A: Thermodynamic assessment of the Cu-B system supported by key experiment and first-principles calculations. Journal of Phase Equilibria and Diffusion. 2009; **30** (5): 480–486

[34] Morishita M, Koyama K, Yagi S, Zhang G: Calculated phase diagram of Ni-Mo-B ternary system. Journal of Alloys Compounds. 2001; **314** (1–2): 212–218.

[35] Cao W, Chen SL, Zhang F, Wu K, Yang Y, Chang YA, Schmid-Fetzer R, Oates WA: PANDAT software with panEngine, panoptimizer and panprecipitation for multi-component phase diagram calculation and materials property simulation. Computer Coupling of Phase Diagrams and Thermochemistry. 2009; **33** (2): 328–342

[36] Guillermet AF: An assessment of the Fe-Mo system. Computer Coupling of Phase Diagrams and Thermochemistry. 1982; **6** (2): 127–140.

[37] Frisk K: Thermodynamic evaluation of the Mo-Ni system. Computer Coupling of Phase Diagrams and Thermochemistry. 1990; **14** (3): 311–320.

[38] Miettinen J, Vassilev G: Thermodynamic Description of Ternary Fe-B-X Systems. Part 2: Fe-B-Ni. Archives of Metallurgy and Materials. 2014; **59**: (2): 609–614.

[39] Gladyshevsky EI, Fedorov TF, Kuzma Yu.B, Skolozdra RV: Isothermal section of the Molybdenum-Iron-Boron system. Poroshkovaya Metallurgiya.1966; **5**: 305–310.

[40] Haschke H, Nowotny H, Benesovsky F: Untersuchungen in den dreistoffen: (Mo-W)-(Fe,Co,Ni) - B. Monatshefte Chemie. 1966; **97**: 1459–1468.

[41] Hillert M, Jarl M: A model for alloying effects in ferromagnetic metals. Computer Coupling of Phase Diagrams and Thermochemistry. 1978; **2**: 227–238.

[42] Karwan-Baczewska J: Sintered alloys based on iron powder with boron. AGH University of Science and Technology Press, Cracow, Poland, 2008. pp. 71–75 and pp. 116–117.

IntechOpen